environmental microbiology

Environmental Microbiology (2018) **20**(12), 4503–4511 doi:10.1111/1462-2920.14388

Novel energy conservation strategies and behaviour of *Pelotomaculum schinkii* driving syntrophic propionate catabolism

Catalina A. P. Hidalgo-Ahumada,[1†] Masaru K. Nobu,[2†*] Takashi Narihiro,[2] Hideyuki Tamaki,[2] Wen-Tso Liu,[3] Yoichi Kamagata,[2] Alfons J M Stams,[1,4] Hiroyuki Imachi[5*] and Diana Z Sousa[1*]

[1]*Laboratory of Microbiology, Wageningen University & Research, Stippeneng 4, 6708 WE Wageningen, Wageningen, The Netherlands.*

[2]*Bioproduction Research Institute, National Institute of Advanced Industrial Science and Technology (AIST), 1-1-1 Higashi, Tsukuba, Ibaraki, 305-8566, Japan.*

[3]*Department of Civil and Environmental Engineering, University of Illinois at Urbana-Champaign, 205 North Mathews Ave, Urbana, IL, 61801, USA.*

[4]*Center of Biological Engineering, University of Minho, Campus de Gualtar, 4710-057, Braga, Portugal.*

[5]*Department of Subsurface Geobiological Analysis and Research (D-SUGAR), Japan Agency for Marine-Earth Science & Technology (JAMSTEC), Yokosuka, Kanagawa, 237-0061, Japan.*

Summary

Under methanogenic conditions, short-chain fatty acids are common byproducts from degradation of organic compounds and conversion of these acids is an important component of the global carbon cycle. Due to the thermodynamic difficulty of propionate degradation, this process requires syntrophic interaction between a bacterium and partner methanogen; however, the metabolic strategies and behaviour involved are not fully understood. In this study, the first genome analysis of obligately syntrophic propionate degraders (*Pelotomaculum schinkii* HH and *P. propionicicum* MGP) and comparison with other syntrophic propionate degrader genomes elucidated novel components of energy metabolism behind *Pelotomaculum* propionate oxidation. Combined with transcriptomic examination of *P. schinkii* behaviour in co-culture with *Methanospirillum hungatei*, we found that formate may be the preferred electron carrier for *P. schinkii* syntrophy. Propionate-derived menaquinol may be primarily re-oxidized to formate, and energy was conserved during formate generation through newly proposed proton-pumping formate extrusion. *P. schinkii* did not overexpress conventional energy metabolism associated with a model syntrophic propionate degrader *Syntrophobacter fumaroxidans* MPOB (i.e., CoA transferase, Fix and Rnf). We also found that *P. schinkii* and the partner methanogen may also interact through flagellar contact and amino acid and fructose exchange. These findings provide new understanding of syntrophic energy acquisition and interactions.

Originality-Significance Statement

Syntrophic interaction between fatty acid-degrading *Bacteria* and methanogenic *Archaea* is a critical component of methanogenic decomposition of organic compounds. This study reports the first genome and transcriptome analyses of obligately syntrophic propionate oxidizers (e.g., *Pelotomaculum schinkii*). The investigation reveals novel insights into the energy metabolism and interspecies interactions of *P. schinkii* and differences between two well-known syntrophic propionate-oxidizing genera *Syntrophobacter* and *Pelotomaculum.*

Introduction

Syntrophy is a mutualistic microbial interaction, where for energetic reasons the degradation of a substrate can only occur when the reaction products, such as H_2, acetate and formate are consumed by a partner microorganism. Methanogens and sulfate–reducing bacteria serve often as interacting partners of syntrophic bacteria by efficiently consuming their products to low concentrations (McInerney *et al*., 2009). Syntrophy is necessary for the

Received 10 May, 2018; revised 2 August, 2018; accepted 15 August, 2018. *For correspondence. E-mail m.nobu@aist.go.jp; Tel. +81-29-861-6591; Fax +81-29-861-6587. E-mail imachi@jamstec.go.jp; Tel. +81-46-867-9709; Fax +81-46-867-9715. E-mail diana.sousa@wur.nl; Tel. +31217483317.

†These authors contributed equally to this work.

degradation of alcohols, organic acids and aromatic compounds in methanogenic ecosystems and is thus important in the global carbon cycle (McInerney *et al*., 2009; Schink and Stams, 2013). Degradation of propionate is thermodynamically a challenging conversion [ΔG = +73.8 kJ $mol_{propionate}$, for H_2 generation at 37°C and pH 7 (Thauer *et al*., 1977; Hanselmann, 1991; Amend and Shock, 2001)]. Although any bacterium requires a reaction to have at least −15 kJ mol^{-1} to harness energy, the above propionate degradation can only reach this when H_2 (or formate) is kept at a low concentration (2.85 Pa H_2 or 1.58 μM formate) at 37°C, pH 7, 1 mM propionate, 1 mM acetate and 50 mM HCO_3^-. Thus, syntrophic propionate degraders must cope with highly energy-constrained conditions (Scholten *et al*., 2000; Adams *et al*., 2006).

Only four bacterial genera are known to syntrophically degrade propionate: *Syntrophobacter*, *Pelotomaculum*, *Smithella* and *Desulfotomaculum* (Harmsen *et al*., 1993; Wallrabenstein *et al*., 1995; Harmsen *et al*., 1998; Chen *et al*., 2005; de Bok *et al*., 2005). Biochemical and genomic analyses of *Syntrophobacter fumaroxidans* MPOB (Harmsen *et al*., 1998) and *Pelotomaculum thermopropionicum* SI (Imachi *et al*., 2002) have provided insight into their thermodynamically optimized way of life. This includes the discovery of use of energy from exergonic reactions and proton motive force to drive parallel endergonic reactions (i.e., energy conservation and reverse electron transport respectively; Houwen *et al*., 1990; Kosaka *et al*., 2008; Plugge *et al*., 2012; Sieber *et al*., 2012) and close physical interaction with the partner methanogen (Shimoyama *et al*., 2009; Stams and Plugge, 2009; Felchner-Zwirello *et al*., 2013). These studies have been instrumental to the development of our understanding of syntrophic propionate oxidation. However, *S. fumaroxidans* MPOB and *P. thermopropionicum* SI are not obligately syntrophic and can live as fermenters and/or sulfate reducers, so the biochemical and thermodynamic strategies and behaviour of species dedicated to syntrophy remain to be explored [e.g., *P. schinkii* HH and *P. propionicicum* MGP (de Bok *et al*., 2005; Imachi *et al*., 2007)].

In this study, we sequenced the first genomes of obligately syntrophic organisms *P. schinkii* HH and *P. propionicicum* MGP, sequenced an additional *Pelotomaculum* sp. for comparison (*P.* sp. FP), analysed their propionate oxidation and electron transfer strategies, and compared these genomes with other syntrophic propionate-degraders (SPDs). To further investigate the behaviour of an obligate syntrophic organism, we examined the gene expression of *P. schinkii* HH in co-culture with *Methanospirillum hungatei* JF-1 through transcriptomics. In total, we describe novel energy conservation strategies and interactions for *Pelotomaculum* SPDs and differences between *Pelotomaculum* and *Syntrophobacter.*

Results and Discussion

General genome information and the propionate oxidation pathway

The sequenced genomes of *Pelotomaculum* spp. (*P. schinkii* HH, *P. propionicum* MGP and *P.* sp. FP) were 3.95–4.47 Mb in size (sequencing depth of 69–122× coverage), had a GC content of 49.8%–50.8%, and harboured 3847–4302 coding sequences (Supporting Information Table S1). All genomes are available under NCBI BioProject PRJNA454509. All genomes encoded the conventional propionate oxidation pathway: propionate uptake, propionate activation to propionyl-CoA, carboxylation to methylmalonyl-CoA, subsequent isomerization to succinyl-CoA, oxidative decarboxylation to acetyl-CoA via oxaloacetate and pyruvate, acetyl-CoA dethiolation to acetate, and acetate export (Fig. 1; Supporting Information Table S3). While the first two steps (propionate activation and propionyl-CoA carboxylation) required energy input, these *Pelotomaculum* spp. all encoded CoA transferases and carboxyltransferases to couple the energy-requiring (i.e., endergonic) steps with downstream energy-yielding (i.e., exergonic) steps: acetyl-CoA dethiolation and oxaloacetate decarboxylation

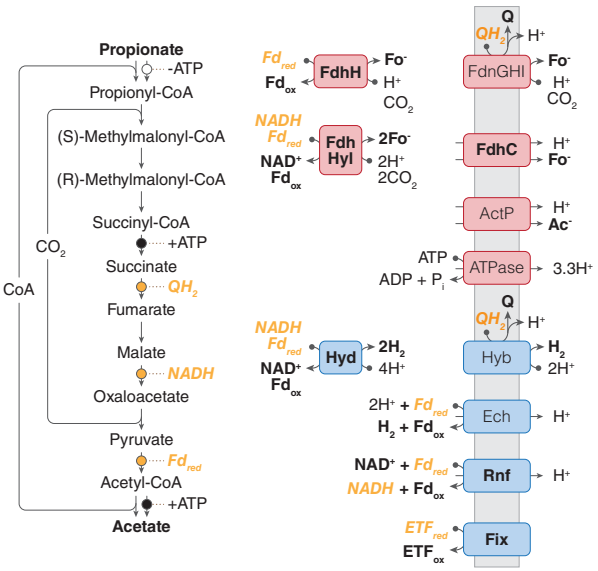

Fig. 1. Propionate degradation pathway of *Pelotomaculum schinkii* HH. Enzyme complexes involved in energy conservation, H_2 metabolism, or formate metabolism are coloured based on whether they were among the top 100 genes (red) or not (blue) in terms of gene expression (RPKM). The reduced electron carriers responsible for transducing reducing power from propionate oxidation to H_2 and formate generation are highlighted (orange). Enzymes related to H_2 and formate metabolism found across all sequenced syntrophic propionate degraders genomes are bolded.

respectively. All species also encoded AMP-dependent acyl-CoA synthetases to activate propionate and dethiolate acetyl-CoA independently. Based on these features, propionate oxidation to acetate by these *Pelotomaculum* spp. might yield 1 mol ATP and $6e^-$ (1 mol each of NADH, reduced ferredoxin (Fd_{red}) and menaquinol) per mol propionate.

Electron transfer proteins

Under methanogenic conditions, favourable electron acceptors are unavailable for electron disposal. Syntrophic organisms like *Pelotomaculum* spp. must resort to using H^+ and CO_2 as electron sinks for the reducing power generated from substrate oxidation (e.g., NADH, Fd_{red} and menaquinol). This is quite challenging as H^+ reduction to H_2 and CO_2 reduction to formate both have very low reduction potentials (E' = −420 mV). For example, NADH (E' = −230 mV) is a highly unfavourable donor for H^+/CO_2 reduction. To overcome this thermodynamic obstacle, all *Pelotomaculum* spp. encoded confurcating hydrogenases and formate dehydrogenases capable of driving endergonic H_2/formate-generating NADH oxidation using exergonic H_2/formate-generating oxidation of Fd_{red} (E' = −430 mV; Fig. 1 and Supporting Information Table S3). Electron confurcation systems have also been described for other syntrophic organisms (de Bok *et al*., 2003; McInerney *et al*., 2007; Kosaka *et al*., 2008; Sieber *et al*., 2010). Strains HH and FP also encoded membrane-bound hydrogenases (Ech) that can directly oxidize Fd_{red}, taking advantage of the positive energy margin between Fd_{red} and H_2 and extruding protons to conserve energy in the form of proton motive force.

As for menaquinol oxidation, all studied *Pelotomaculum* spp. encoded cytochrome b-linked quinone-dependent hydrogenases (HybABCO) and formate dehydrogenases (FdnGHI and FdnG-HybAB). We found that, in all *Pelotomaculum* spp., the cytochrome b subunits (i.e., HybB and FdnI) had quinone-binding sites on the periplasmic side [quinone-binding domain (Fisher and Rich, 2000) on periplasmic end of transmembrane helix (Kall *et al*., 2004)], indicating that Hyb- and Fdn-mediated menaquinol re-oxidation could potentially release protons on the periplasmic side and contribute to proton motive force formation. This is contrasting to the well-characterized *Escherichia coli* FdnGHI that has a cytoplasm-oriented quinone-binding site and couples formate oxidation with proton extrusion (Jormakka *et al*., 2002). Further, the *Pelotomaculum* coupling of menaquinol-oxidizing H_2/formate generation with proton extrusion is quite surprising as menaquinone has a much less negative reduction potential (E' = −74 mV) than H^+ and CO_2. Energy acquisition from menaquinol oxidation would be a highly valuable biochemical strategy for syntrophic organisms, but simple thermodynamic calculations cannot justify this reaction, which is endergonic (ΔG = +38.20 kJ mol^{-1}) even if the H_2 concentration were as low as 1 Pa (or 2.96 μM formate based on equilibrium at 37°C with 0.3 atm CO_2). Perhaps these *Pelotomaculum* spp. Hyb and Fdn employ an unbeknownst anaerobic energy conservation strategy.

While both H_2 and formate are known to play a critical role in syntrophic electron transfer, several studies have reported that SPDs may prefer formate transfer (Schmidt and Ahring, 1995; de Bok *et al*., 2002). For example, *P. schinkii* could not grow in co-culture with a methanogen incapable of utilizing formate (de Bok *et al*., 2005). Unlike H_2, formate is an anion, so it cannot freely pass the cell membrane and will inevitably accumulate in the cytosol. To address this, all studied *Pelotomaculum* spp. encoded potential formate transporters (FdhC) related (> 40% amino acid similarity) to *Escherichia coli* and *Methanobacterium formicicum* formate transporters FocA and FdhC (White and Ferry, 1992; Suppmann and Sawers, 1994; Supporting Information Table S3). We suspect that FdhC can take advantage of an accumulating formate gradient and couple formate extrusion to the symport of protons with generation of proton motive force. In agreement, the FdhC were adjacent to the electron-confurcating formate dehydrogenases FdhAB-HylABC in the genomes of *P. schnkii* and *P.* sp. FP. This is a novel energy conservation mechanism for syntrophic propionate degradation.

The studied *Pelotomaculum* spp. also encoded energy-conserving enzymes that can potentially mediate electron transfer from propionate oxidation to H_2/formate generation. *P. schinkii* and *P.* sp. FP encoded Fd:NADH oxidoreductases (RnfABCDEG) that can couple exergonic electron transfer from Fd_{red} to NAD^+ with proton extrusion. In addition, all studied *Pelotomaculum* spp. harboured electron transfer flavoprotein dehydrogenases (FixABCX) that can couple quinol-reducing electron transfer flavoprotein oxidation with proton pumping. Both complexes have been proposed to play key roles in syntrophic metabolism (Sieber *et al*., 2012; Nobu *et al*., 2015). In total, each of these *Pelotomaculum* spp. possessed at least five potential approaches to pairing electron transfer with proton motive force generation, which suggests metabolic optimization towards energy conservation.

Comparison with other syntrophic propionate degraders

Besides the three mesophilic *Pelotomaculum* strains discussed so far, two other SPDs have been genomically characterized by previous studies: thermophilic *Pelotomaculum thermopropionicum* and mesophilic *Syntrophobacter fumaroxidans* (Kosaka *et al*., 2008; Plugge *et al*., 2012). All these SPDs had the general propionate

oxidation pathway, electron-confurcating hydrogenase, electron-confurcating formate dehydrogenase, monomeric formate dehydrogenase (FdhH), and formate transporter in common (Supporting Information Table S3). This suggests that electron confurcation and the newly proposed energy acquisition from formate extrusion are core features of syntrophic propionate degradation. *P. thermopropionicum* also shares many other features (e.g., quinone-dependent hydrogenases and formate dehydrogenases) with the three mesophilic *Pelotomaculum* strains, but lacks Ech and Rnf (Supporting Information Table S3). As *S. fumaroxidans* is from a different genus, we found several major differences. While the four *Pelotomaculum* spp. only encoded propionyl-CoA:acetate CoA transferases, *S. fumaroxidans* also harboured a propionyl-CoA:succinate CoA transferase. Thus, unlike *Pelotomaculum*, *Syntrophobacter* may also activate propionate using succinyl-CoA hydrolysis as an energy input. Conversely, *Syntrophobacter* lacked membrane-bound hydrogenases (Ech and HybABCO) and formate dehydrogenases (FdnGHI) associated with proton extrusion, and rather encoded a cytosolic NiFe hydrogenase (HoxEFUHY) and periplasmic heterodimeric formate dehydrogenase that were not directly involved in proton pumping. The energy conservation strategies of *Pelotomaculum* and *Syntrophobacter* clearly differ, where *Syntrophobacter* seemed to have a more intricate energy conservation mechanism. A recent study has also reported contrasting energy conservation mechanisms among syntrophic acetate and aromatic compound oxidizers (Nobu *et al*., 2017; Manzoor *et al*., 2018), suggesting diversity in energy metabolism across syntrophic organisms.

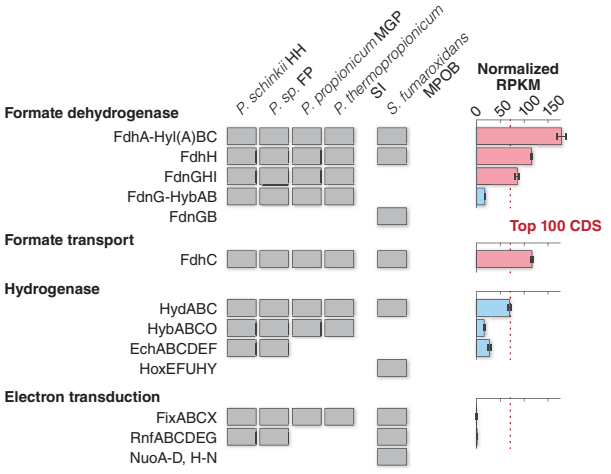

Fig. 2. Energy conservation strategies of *Pelotomaculum* and *Syntrophobacter* species (left) and gene expression of these enzymes by *P. schinkii* HH under co-culture with *Methanospirillum hungatei* JF-1 (right). The gene expression of the subunit with the highest expression level is shown as RPKM (reads per kilobase of transcript per million mapped reads) normalized to the *P. schinkii*'s median RPKM. Bars are coloured based on whether the subunits have expression levels (RPKM) among the top 100 genes (red) or not (blue). Error bars are also shown.

Pelotomaculum schinkii gene expression during syntrophic propionate degradation

To further investigate the energy conservation strategies of syntrophic propionate degradation, we studied the gene expression profile of a co-culture of an obligate SPD (*P. schinkii*) and H_2/formate-using methanogen *M. hungatei.* Transcriptomes were sequenced for triplicate co-cultures (4.9–5.2 million reads and 736–778 Gb) and, as a reference, triplicate cultures of *M. hungatei* as well (3.8–4.7 million reads and 577–704 Gb; Supporting Information Table S2). For the co-cultures, 22.2%–26.9% and 7.6%–11.2% of the transcriptomic reads mapped to *P. schinkii* and *M. hungatei* CDS respectively. For the *M. hungatei* pure culture, 35.1%–51.3% mapped to *M. hungatei* CDS. While most *P. schinkii* genes involved in propionate uptake, propionate oxidation, and acetate export were highly expressed (3rd–81st on the expression ranking, refer to Supporting Information Table S3 for specific gene expression levels and standard deviation), CoA transferases ranked very low (2367th and below; Supporting Information Table S3). Instead, *P. schinkii* expressed an AMP-dependent acyl-CoA synthetase (Acs1; 181st). Thus, *P. schinkii* likely decouples propionate activation and acetyl-CoA hydrolysis and does not conserve energy here. This is quite dissimilar from other characterized SPDs who are thought to depend on energy conservation via CoA transferases: *Syntrophobacter fumaroxidans* and *Pelotomaculum thermopropionicum* (Kato *et al*., 2009; Plugge *et al*., 2012). Clearly, even strategies for propionate oxidation can vary, suggesting overlooked diversity among SPDs in thermodynamic optimization. The use of AMP-dependent pyrophosphate-forming acyl-CoA synthetase for substrate activation has also been observed for *Syntrophus aciditrophicus* during syntrophic benzoate degradation, indicating that *P. schinkii* shares similarities in biochemical strategies with other syntrophic organisms. In addition, like *S. aciditrophicus* and *Clostridium ultunense* (James *et al*., 2016; Manzoor *et al*., 2018), *P. schinkii* may conserve energy from substrate activation by coupling proton extrusion with hydrolysis of the byproduct pyrophosphate via a membrane-bound pyrophosphatase (rank 342nd; Supporting Information Table S4).

The gene expression profile of electron transfer enzymes also revealed unexpected behaviour. *P. schinkii* highly expressed formate generation through three formate dehydrogenases: FdhAB-HylABC (27th), FdhH (59th) and FdnGHI (86th; Figs. 1 and 2; Supporting Information Table S3). Conversely, the hydrogenases all

had lower expression levels (all ranked less than 100th). To compare, the electron-confurcating and quinone-dependent hydrogenase catalytic subunits only had 48.5 ± 1.8% (p = 0.011) and 17.8 ± 1.1% (p = 0.002) of the expression of the respective formate dehydrogenase catalytic subunits. This suggests that *P. schinkii* may preferentially funnel reducing power into CO_2-reducing formate generation rather than H_2 production, like *S. fumaroxidans* and *P. thermopropionicum* (Worm *et al*., 2011; Liu and Lu, 2018). In particular, the markedly different expression levels of Hyb and Fdn indicates that *P. schinkii* primarily re-oxidizes menaquinol through formate generation. This is the first evidence for a syntrophic organism segregating different electron carriers towards different electron acceptors. To complement the highly active formate metabolism, *P. schinkii* also highly expressed the formate transporter (FdhC; 58th) to acquire energy through the newly proposed formate export. This further evidences the importance of formate-mediated proton pumping for syntrophic propionate degradation (Fig. 2). Similarly, the methanogenic partner *M. hungatei* in the co-culture expressed formate uptake (FdhC, Mhun_1811; 13th) and oxidation (two FdhAB, Mhun_1813–14 and Mhun_3238–37; 19th and 23rd) higher than H_2 oxidation (e.g., FrhABDG; 40th). The *M. hungatei* formate dehydrogenase expression level was significantly higher when grown in co-culture than in an H_2-fed axenic culture (14.54×, p = 0.05; Supporting Information Tables S5 and S6), indicating that *M. hungatei* was oxidizing *P. schinkii*-derived formate.

Interestingly, the highly expressed formate dehydrogenases can directly transfer electrons from propionate oxidation to formate generation. Propionate oxidation to acetate generates NADH, Fd_{red} and menaquinol as reducing equivalents at a 1:1:1 ratio (Fig. 1). The expressed formate dehydrogenases can stoichiometrically re-oxidize these electron carriers: FdhAB-HylABC putatively oxidizes NADH and Fd_{red} at a 1:1 ratio and FdnGHI oxidizes menaquinol, using CO_2 as an electron acceptor. This is quite unique as syntrophic organisms typically depend on electron transduction mechanisms to couple substrate degradation with electron disposal (e.g., NADH:Fd oxidoreductase Rnf and electron transfer flavoprotein dehydrogenase Fix; Sieber *et al*., 2012). The genome of *P. schinkii* encoded such syntrophy-associated enzymes (Rnf and Fix) but did not express them highly (Rnf 1863rd and Fix 3095th; Supporting Information Table S3). Another syntrophic organism, *Syntrophaceticus schinkii*, has also been reported to possess but not express Rnf (Manzoor *et al*., 2016). Thus, *P. schinkii*, and perhaps other syntrophic organisms, employ a minimalist energy conservation approach distinct from those that are well-characterized (e.g., *Syntrophobacter fumaroxidans* and *Syntrophus aciditrophicus*; McInerney *et al*., 2007; Plugge *et al*., 2012).

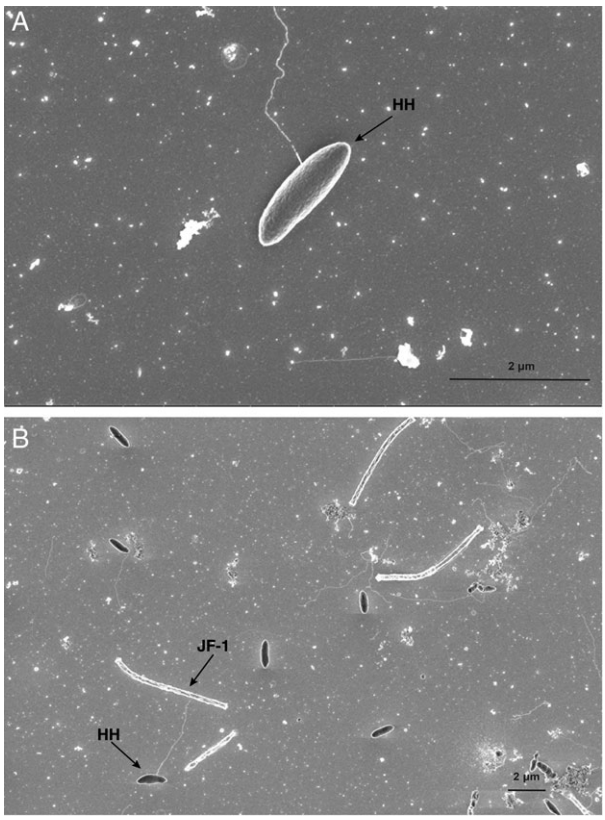

Fig. 3. Scanning electron microscopy (SEM) of *P. schinkii* HH with a radial flagellum (A) and in contact with *M. hungatei* JF-1 via flagellum (B).

Flagellum and amino acid-mediated syntrophy. We further explored genomes and the transcriptome for noncatabolic behaviour relevant to syntrophy. Previous studies demonstrate that *P. thermopropionicum* can interact with its partner methanogen through flagella (Ishii *et al*., 2005; Shimoyama *et al*., 2009; Liu and Lu, 2018). We also found that *P. schinkii* expressed flagella-related genes despite being immotile (average rank 484th; Supporting Information Table S3; Fig. 3; de Bok *et al*., 2005). Given that all *Pelotomaculum* SPDs encoded complete flagellum biosynthesis machinery (Supporting Information Table S3), 'flagellum-mediated symbiosis' may be a core mechanism for *Pelotomaculum*-initiated syntrophy. While most flagellar components were quite homologous between *Pelotomaculum* SPDs (average amino acid sequence similarity > 60%), the specific subunit that interacts with methanogens [FliD (Shimoyama *et al*., 2009)] can be quite different between strains (HH-SI 29.7%, HH-MGP 45.4% and HH-FP 97.0%). Though highly speculative, perhaps FliD (and thus *Pelotomaculum*) may have some level of specificity or affinity to methanogenic partner. In future work, it would be interesting to delve into investigation of the stimuli behind such interspecies interactions and the importance in H_2 and formate transfer.

The transcriptomics also revealed potential nutrient exchange between *P. schinkii* and *M. hungatei.* Although

P. schinkii had complete pathways for synthesizing all standard amino acids (AAs), it had depressed expression of biosynthesis for five AAs (i.e., lower than median gene expression; Fig. 4). Conversely, we found that *M. hungatei* expressed synthesis for three of these AAs (arginine, tyrosine and methionine; greater than median gene expression). Similarly, *P. schinkii* highly expressed biosynthesis of four other AAs that *M. hungatei* did not (proline, serine, phenylalanine and tryptophan). *M. hungatei* indeed increased expression of arginine and methionine synthesis and decreased expression of tryptophan synthesis in co-culture compared to axenic, providing evidence for changes in AA biosynthesis behaviour in the presence of *P. schinkii.* This suggests division of labour for AA biosynthesis and AA exchange between the two syntrophically interacting strains. However, these results must be interpreted with caution as the co-culture contains yeast extract, which contains amino acids. Some recent studies also identify coordinated cross-feeding between organisms (Hubalek *et al*., 2017; Liu *et al*., 2018; Zengler and Zaramela, 2018), suggesting nutrient exchange may be a prevalent and critical interaction for syntrophy.

Other anaerobic metabolism. P. schinkii is reported to syntrophically degrade propionate and also co-utilize fumarate in the presence of propionate, but not metabolize any other tested compounds (de Bok *et al*., 2005). However, *P. schinkii* genome encoded genes for the degradation of many amino acids, fructose and ethanol and fermentative production of butyrate, lactate, ethanol and propanediol (Supporting Information Table S7). Interestingly, catabolism-specific pathways of fructose (using phosphofructokinase rather than anabolic fructose-1,6-bisphosphatase) and branched-chain AAs were highly expressed by *P. schinkii* (all genes have average RPKM greater than the median RPKM for *Pelotomaculum*; Supporting Information Table S7) while biosynthesis of these compounds were expressed by *M. hungatei* (average RPKM normalized to the median: 1.01–15.07 for fructose and 2.56–24.97 for branched-chain AAs). This suggests that exchange of these compounds may also play a role in syntrophy between the two partners and, unlike AA transfer discussed in the previous section, fructose and branched-chain AAs may serve as a supplementary energy sources co-utilized with propionate. While aspartate and alanine metabolism were also highly expressed, these pathways are reversible and may be used for anabolism. Most other catabolism- (i.e., threonine, methionine and lysine degradation) or fermentation-specific (i.e., ethanol, lactate, butyrate and propanediol metabolism) pathways were not highly expressed (Supporting Information Table S7). Given that *P. schinkii* was reported to not be able to utilize or produce (in excess) these compounds (de Bok *et al*., 2005), *P. schinkii* may employ these genes for other untested environmental conditions and/or alternative lifestyles that we have yet to uncover.

As syntrophic propionate catabolism only has a small energy margin (−15 kJ mol^{-1}) that can be shared between the syntroph and its partner (de Bok *et al*., 2004; Schink and Stams, 2013), it is critical for SPD genera to optimize the energetics. Comparative genomics and transcriptomics revealed that *Pelotomaculum* syntrophy entails formate-dominated interspecies electron transfer, energy acquisition through formate extrusion, potential flagellum-mediated interaction, exchange of AA for anabolism, exchange of AA and fructose for potentially supplementary catabolism and unexpected independence from conventional energy conservation pathways typically associated with other well-studied syntrophs (e.g., *Syntrophobacter fumaroxidans*, *Syntrophomonas wolfei* and *Syntrophus aciditrophicus*; McInerney *et al*., 2007; Sieber *et al*., 2010; Plugge *et al*., 2012; Sieber *et al*., 2012). Most importantly, these results reinforce a previous observation that formate may play a larger role in syntrophy than H_2 (de Bok *et al*., 2002) and provide further evidence for cross-feeding between syntrophs and their partners in parallel with H_2 and formate transfer.

Methods

Cultivation experiment. M. hungatei JF-1^T (=DSM 864^T) was obtained from the Deutsche Sammlung von Mikroorganismen and Zellkulturen (Braunschweig, Germany). The co-culture of *P. schinkii* and *M. hungatei* was obtained from internal strain collection. A bicarbonate-buffered mineral medium was used, with the following composition: 3 mM Na_2HPO_4, 3 mM KH_2PO_4, 5.6 mM NH_4Cl, 0.75 mM $CaCl_2$, 0.5 mM $MgCl_2$, 5 mM NaCl, 50 mM $NaHCO_3$, 1 mM Na_2S, 7.5 mM $FeCl_2$, 1 mM H_3BO_3, 0.5 mM $ZnCl_2$, 0.1 mM $CuCl_2$, 0.5 mM $MnCl_2$, 0.5 mM $CoCl_2$, 0.1 mM $NiCl_2$, 0.1 mM Na_2SeO_3, 0.1 mM Na_2WO_4, 0.1 mM Na_2MoO_4, 0.5 mg

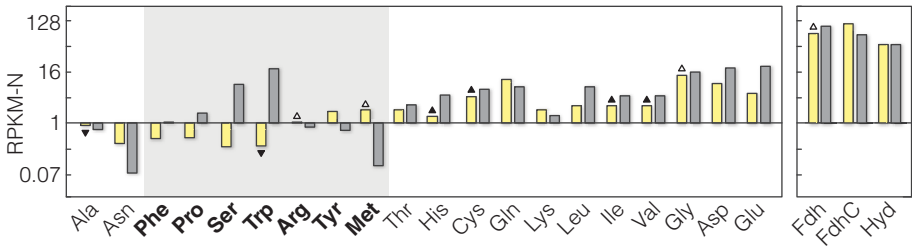

Fig. 4. Expression of amino acid biosynthesis, formate metabolism (Fdh), formate transport (FdhC) and H_2 metabolism (Hyd), by *M. hungatei* JF-1 (yellow) and *P. schinkii* HH (grey). The expression level of the gene with the lowest expression level (RPKM normalized to the median RPKM of the corresponding genome) of each pathway is shown. Biosynthesis pathways with significantly different expression levels ($p \leq 0.05$) between co-culture and axenic culture for *M. hungatei* JF-1 are marked (black triangle). Pathways are marked with a white triangle if the expression levels are significantly different only when axenic culture replicate 2 is excluded. The direction of the triangle indicates whether *M. hungatei* JF-1's expression increases (up) or decreases (down) in the co-culture compared to the axenic culture.

EDTA l^{-1} and the following vitamins (mg l^{-1}): 0.02 biotin, 0.2 nicotinic acid, 0.5 pyridoxine, 0.1 riboflavin, 0.2 thiamin, 0.1 cyanocobalamin, 0.1 p-aminobenzoic acid, 0.1 pantothenic acid, 0.1 lipoic acid and 0.1 folic acid. To obtain the biomass for genomic sequencing, *M. hungatei* was cultured at 37°C in 1 l serum bottles with 500 ml medium and a gas phase of 1.7 atm 80:20 v/v of H_2/CO_2. The *P. schinkii* co-culture was inoculated into a pregrown *M. hungatei* culture (1:10). Prior to inoculation, CH_4 and H_2 was removed by exchanging with 1.7 atm of N_2/CO_2 gas (80:20 v/v) and 0.1 g/l of yeast extract and 20 mM of propionate was added. Co-culture bottles were done in triplicates and incubated at 37°C during approximately 30 days. For transcriptome sequencing, 10% of co-culture inoculum was transferred directly to 500 ml bottles with 250 ml medium and incubated at 37°C during approximately 15 days. Pure cultures of *M. hungatei* were grown at 37°C during 4 days in 250 ml bottles with 100 ml medium and 1.7 atm 80:20 v/v of H_2/CO_2 in the headspace. All culturing and sequencing for transcriptomics was done in biological triplicates.

Nucleic acids extraction. Biomass was harvested by centrifugation at 15.000 g at 4°C under sterile conditions. DNA was extracted using MasterPure™ Gram Positive DNA Purification Kit following the manufacturer specifications. Quality and quantity of total DNA was measured using a NanoDrop™ 2000 spectrophotometer and Qubit™ dsDNA BR Assay Kit. Total RNA extraction was performed from cells harvested in the middle of exponential growth phase (~6 mM CH_4 produced and 10 mM propionate consumed). Lysis and protein precipitation was performed using the solutions and enzymes from MasterPure™ Gram Positive DNA Purification Kit as follows: Lysozyme incubation at room temperature for 10 min, after lysis 3 uL of β-mercaptoethanol were added, cells were sonicated using Bendelin SONOPULS HD 3200 ultrasonic homogenizer (6 cycles of 20 s. pulse 30 s. pause) and proteinase K incubation at 60°C for 10 min. Protein precipitation was performed according to the kit specifications. Automated RNA purification was performed using Maxwell® 16 MDx instrument and LEV simplyRNA Purification Kit (DNAse treatment and 16S rRNA depletion was included on the kit).

Microscopy. For scanning electron microscopy analysis, the culture was adhered to poly L-lysin 12 mm coated coverslips (Corning, BioCoat) and incubated for 1 h at room temperature. The cells were then fixed in 2.5% glutaraldehyde in 0.1 M phosphate buffer (pH 7.4) for 1 h at room temperature, rinsed 3 times with 0.1 M phosphate buffer (pH 7.4) and postfixed with 1% osmium tetroxide for 60 min. Hereafter, the cells were dehydrated in a graded alcohol series (10%, 30%, 50%, 70%, 80%, 96% and 100%), dried to critic point in 100% ethanol with CO_2 in the Leica EM CPD300 system and mounted onto aluminium stubs and coated with tungsten. Cells were subsequently studied with a FEI Magellan 400 scanning electron microscope.

Sequencing and bioinformatics. To sequence the genomes of *P. schinkii*, *P. propionicum* and *P.* sp. FP, we performed DNA extraction, Illumina (San Diego, CA, USA) MiSeq sequencing, quality control with Trimmomatic v0.36 (SLIDINGWINDOW:6:30 MINLEN:78 LEADING:3 TRAILING:3; Bolger *et al*., 2014), and genome assembly with SPAdes v3.11 as previously described (Narihiro *et al*., 2016a,b). For the *P. schinkii* and *M. hungatei* co-culture, genomic DNA was also sequenced using PacBio (PacBio RS II, > 6000 bp reads, 500 Mb raw data), and the resulting sequences were co-assembled using SPAdes v3.10 with default settings. The *M. hungatei* sequences were removed by comparison with the publically available *M. hungatei* genome. The *Pelotomaculum* genomes were annotated using Prokka 1.12 (Seemann, 2014; Nobu *et al*., 2015). As for the transcriptomics, RNA extracted from the *P. schinkii* and *M. hungatei* co-culture was sequenced using RNA-seq strand specific library constructed using a Kapa Hyper Prep Kit (Kapa Biosystems) including 16S depletion and subjected to 250–300 bp insert paired-end sequencing on an Illumina HiSeq 4000 platform (sequenced by Beijing Novogene Bioinformatics Technology), trimmed using Trimmomatic v0.36 (SLIDINGWINDOW:6:30 MINLEN:50 LEADING:3 TRAILING:3), and mapped to the *P. schinkii* and *M. hungatei* genomes using the Burrows Wheeler Aligner with default settings (Li and Durbin, 2009) to calculate gene expression levels as previously described (Nobu *et al*., 2017).

Acknowledgements

We thank Steven Aalvink for scanning electron microscopy analysis and WEMC for making the system available. The research leading to these results has received funding from the European Research Council under the European Union's Seventh Framework Programme (FP/2007-2013) / ERC Grant Agreement n. [323009] and a Gravitation Grant (Project 024.002.002) of the Netherlands Ministry of Education, Culture and Science and the Netherlands Organisation for Scientific Research (NWO). This work was also supported by The Japan Society for the Promotion of Science with Grant-in-Aid for Scientific Research No. 18H03367 to MK Nobu and 17H05239 and 18H01576 to T Narihiro.

References

Adams, C. J., Redmond, M. C., and Valentine, D. L. (2006) Pure-culture growth of fermentative Bacteria, facilitated by H_2 removal: bioenergetics and H_2 production. *Appl Environ Microbiol* **72**: 1079–1085.

Amend, J. P., and Shock, E. L. (2001) Energetics of overall metabolic reactions of thermophilic and hyperthermophilic *Archaea* and *Bacteria*. *FEMS Microbiol Rev* **25**: 175–243.

de Bok, F. A., Luijten, M. L., and Stams, A. J. (2002) Biochemical evidence for formate transfer in syntrophic propionate-oxidizing cocultures of *Syntrophobacter fumaroxidans* and *Methanospirillum hungatei*. *Appl Environ Microbiol* **68**: 4247–4252.

de Bok, F. A., Hagedoorn, P. L., Silva, P. J., Hagen, W. R., Schiltz, E., Fritsche, K., and Stams, A. J. (2003) Two W-containing formate dehydrogenases (CO_2-reductases) involved in syntrophic propionate oxidation by *Syntrophobacter fumaroxidans*. *Eur J Biochem* **270**: 2476–2485.

de Bok, F. A., Plugge, C. M., and Stams, A. J. (2004) Interspecies electron transfer in methanogenic propionate degrading consortia. *Water Res* **38**: 1368–1375.

de Bok, F. A. M., Harmsen, H. J. M., Plugge, C. M., de Vries, M. C., Akkermans, A. D. L., de Vos, W. M., and Stams, A. J. M. (2005) The first true obligately syntrophic propionate-oxidizing bacterium, *Pelotomaculum schinkii* sp nov., co-cultured with *Methanospirillum hungatei*, and emended description of the genus *Pelotomaculum*. *Int J Syst Evol Microbiol* **55**: 1697–1703.

Bolger, A. M., Lohse, M., and Usadel, B. (2014) Trimmomatic: a flexible trimmer for Illumina sequence data. *Bioinformatics* **30**: 2114–2120.

Chen, S. Y., Liu, X. L., and Dong, X. Z. (2005) *Syntrophobacter sulfatireducens* sp. nov., a novel syntrophic, propionate-oxidizing bacterium isolated from UASB reactors. *Int J Syst Evol Microbiol* **55**: 1319–1324.

Felchner-Zwirello, M., Winter, J., and Gallert, C. (2013) Interspecies distances between propionic acid degraders and methanogens in syntrophic consortia for optimal hydrogen transfer. *Appl Microbiol Biotechnol* **97**: 9193–9205.

Fisher, N., and Rich, P. R. (2000) A motif for quinone binding sites in respiratory and photosynthetic systems. *J Mol Biol* **296**: 1153–1162.

Hanselmann, K. W. (1991) Microbial energetics applied to waste repositories. *Experientia* **47**: 645–687.

Harmsen, H. J., Wullings, B., Akkermans, A. D., Ludwig, W., and Stams, A. J. (1993) Phylogenetic analysis of *Syntrophobacter wolinii* reveals a relationship with sulfate-reducing bacteria. *Arch Microbiol* **160**: 238–240.

Harmsen, H. J., Van Kuijk, B. L. M., Plugge, C. M., Akkermans, A. D. L., De Vos, W. M., and Stams, A. J. M. (1998) Syntrophobacter fumaroxidans sp. nov., a syntrophic propionate-degrading sulfate-reducing bacterium. *Int J Syst Bacteriol* **48**: 1383–1387.

Houwen, F. P., Plokker, J., Stams, A. J. M., and Zehnder, A. J. B. (1990) Enzymatic evidence for involvement of the methylmalonyl-CoA pathway in propionate oxidation by *Syntrophobacter wolinii*. *Arch Microbiol* **155**: 52–55.

Hubalek, V., Buck, M., Tan, B., Foght, J., Wendeberg, A., Berry, D., *et al*. (2017) Vitamin and amino acid Auxotrophy in anaerobic consortia operating under methanogenic conditions. *mSystems* **2**: e00038–e00017.

Imachi, H., Sekiguchi, Y., Kamagata, Y., Hanada, S., Ohashi, A., and Harada, H. (2002) *Pelotomaculum thermopropionicum* gen. Nov., sp nov., an anaerobic, thermophilic, syntrophic propionate-oxidizing bacterium. *Int J Syst Evol Microbiol* **52**: 1729–1735.

Imachi, H., Sakai, S., Ohashi, A., Harada, H., Hanada, S., Kamagata, Y., and Sekiguchi, Y. (2007) *Pelotomaculum propionicicum* sp. nov., an anaerobic, mesophilic, obligately syntrophic, propionate-oxidizing bacterium. *Int J Syst Evol Microbiol* **57**: 1487–1492.

Ishii, S., Kosaka, T., Hori, K., Hotta, Y., and Watanabe, K. (2005) Coaggregation facilitates interspecies hydrogen transfer between *Pelotomaculum thermopropionicum* and *Methanothermobacter thermautotrophicus*. *Appl Environ Microbiol* **71**: 7838–7845.

James, K. L., Rios-Hernandez, L. A., Wofford, N. Q., Mouttaki, H., Sieber, J. R., Sheik, C. S., *et al*. (2016) Pyrophosphate-dependent ATP formation from acetyl coenzyme a in *Syntrophus aciditrophicus*, a new twist on ATP formation. *mBio* **7**: e01208–16.

Jormakka, M., Tornroth, S., Byrne, B., and Iwata, S. (2002) Molecular basis of proton motive force generation: structure of formate dehydrogenase-N. *Science* **295**: 1863–1868.

Kall, L., Krogh, A., and Sonnhammer, E. L. (2004) A combined transmembrane topology and signal peptide prediction method. *J Mol Biol* **338**: 1027–1036.

Kato, S., Kosaka, T., and Watanabe, K. (2009) Substrate-dependent transcriptomic shifts in Pelotomaculum thermopropionicum grown in syntrophic co-culture with Methanothermobacter thermautotrophicus. *J Microbial Biotechnol* **2**: 575–584.

Kosaka, T., Kato, S., Shimoyama, T., Ishii, S., Abe, T., and Watanabe, K. (2008) The genome of *Pelotomaculum thermopropionicum* reveals niche-associated evolution in anaerobic microbiota. *Genome Res* **18**: 442–448.

Li, H., and Durbin, R. (2009) Fast and accurate short read alignment with burrows-wheeler transform. *Bioinformatics* **25**: 1754–1760.

Liu, P., and Lu, Y. (2018) Concerted metabolic shifts give new insights into the syntrophic mechanism between propionate-fermenting *Pelotomaculum thermopropionicum* and Hydrogenotrophic *Methanocella conradii*. *Front Microbiol* **9**: 1551.

Liu, Y.-F., Galzerani, D. D., Mbadinga, S. M., Zaramela, L. S., Gu, J.-D., Mu, B.-Z., and Zengler, K. (2018) Metabolic capability and in situ activity of microorganisms in an oil reservoir. *Microbiome* **6**: 5.

Manzoor, S., Bongcam-Rudloff, E., Schnürer, A., and Müller, B. (2016) Genome-guided analysis and whole transcriptome orofiling of the mesophilic syntrophic acetate oxidising bacterium *Syntrophaceticus schinkii*. *PloS ONE* **11**: e0166520.

Manzoor, S., Schnürer, A., Bongcam-Rudloff, E., and Müller, B. (2018) Genome-guided analysis of *Clostridium ultunense* and comparative genomics reveal different strategies for acetate oxidation and energy conservation in syntrophic acetate-oxidising bacteria. *Genes* **9**: 225.

McInerney, M. J., Rohlin, L., Mouttaki, H., Kim, U., Krupp, R. S., Rios-Hernandez, L., *et al*. (2007) The genome of *Syntrophus aciditrophicus*: life at the thermodynamic limit of microbial growth. *Proc Natl Acad Sci USA* **104**: 7600–7605.

McInerney, M. J., Sieber, J. R., and Gunsalus, R. P. (2009) Syntrophy in anaerobic global carbon cycles. *Curr Opin Biotechnol* **20**: 623–632.

Narihiro, T., Nobu, M. K., Tamaki, H., Kamagata, Y., and Liu, W. T. (2016a) Draft genome sequence of *Syntrophomonas wolfei* subsp. *methylbutyratica* strain 4J5T (JCM 14075), a mesophilic butyrate- and 2-methylbutyrate-degrading Syntroph. *Genome Announc* **4**: e00047-16.

Narihiro, T., Nobu, M. K., Tamaki, H., Kamagata, Y., Sekiguchi, Y., and Liu, W. T. (2016b) Comparative genomics of syntrophic branched-chain fatty acid degrading bacteria. *Microbes Environ* **31**: 288–292.

Nobu, M. K., Narihiro, T., Rinke, C., Kamagata, Y., Tringe, S. G., Woyke, T., and Liu, W. T. (2015) Microbial dark matter ecogenomics reveals complex synergistic networks in a methanogenic bioreactor. *ISME J* **9**: 1710–1722.

Nobu, M. K., Narihiro, T., Liu, M., Kuroda, K., Mei, R., and Liu, W. T. (2017) Thermodynamically diverse syntrophic aromatic compound catabolism. *Environ Microbiol* **19**: 4576–4586.

Plugge, C. M., Henstra, A. M., Worm, P., Swarts, D. C., Paulitsch-Fuchs, A. H., Scholten, J. C., *et al*. (2012) Complete genome sequence of *Syntrophobacter fumaroxidans* strain (MPOB(T)). *Stand Genomic Sci* **7**: 91–106.

Schink, B., and Stams, A. J. M. (2013)Syntrophism among prokaryotes . In *The Prokaryotes: Prokaryotic Communities and Ecophysiology*, Rosenberg, E., DeLong, E., Lory, S., Stackebrandt, E., and Thompson, F. (eds). Berlin, Heidelberg: Springer Berlin Heidelberg, pp. 471–493.

Schmidt, J. E., and Ahring, B. K. (1995) Interspecies electron transfer during propionate and butyrate degradation in mesophilic, granular sludge. *Appl Environ Microbiol* **61**: 2765–2767.

Scholten, J. C. M., and Conrad, R. (2000) Energetics of syntrophic propionate oxidation in defined batch and chemostat cocultures. *Appl Environ Microbiol* **66**: 2934.

Seemann, T. (2014) Prokka: rapid prokaryotic genome annotation. *Bioinformatics* **30**: 2068–2069.

Shimoyama, T., Kato, S., Ishii, S., and Watanabe, K. (2009) Flagellum mediates symbiosis. *Science* **323**: 1574–1574.

Sieber, J.R., Sims, D.R., Han, C., Kim, E., Lykidis, A., Lapidus, A.L., *et al*. (2010) The genome of *Syntrophomonas wolfei*: new insights into syntrophic metabolism and biohydrogen production. *Environ Microbiol* **12**: 2289–2301

Sieber, J. R., McInerney, M. J., and Gunsalus, R. P. (2012) Genomic insights into syntrophy: the paradigm for anaerobic metabolic cooperation. *Ann Rev Microbiol* **66**: 429–452.

Stams, A. J., and Plugge, C. M. (2009) Electron transfer in syntrophic communities of anaerobic *Bacteria* and *Archaea*. *Nat Rev Microbiol* **7**: 568–577.

Suppmann, B., and Sawers, G. (1994) Isolation and characterization of hypophosphite--resistant mutants of *Escherichia coli*: identification of the FocA protein, encoded by the pfl operon, as a putative formate transporter. *Mol Microbiol* **11**: 965–982.

Thauer, R. K., Jungermann, K., and Decker, K. (1977) Energy-conservation in chemotrophic anaerobic bacteria. *Bacteriol Rev* **41**: 100–180.

Wallrabenstein, C., Hauschild, E., and Schink, B. (1995) *Syntrophobacter pfennigii* sp. nov., new syntrophically propionate-oxidizing anaerobe growing in pure culture with propionate and sulfate. *Arch Microbiol* **164**: 346–352.

White, W. B., and Ferry, J. G. (1992) Identification of formate dehydrogenase-specific mRNA species and nucleotide sequence of the fdhC gene of *Methanobacterium formicicum*. *J Bacteriol* **174**: 4997–5004.

Worm, P., Stams, A. J., Cheng, X., and Plugge, C. M. (2011) Growth- and substrate-dependent transcription of formate dehydrogenase and hydrogenase coding genes in *Syntrophobacter fumaroxidans* and *Methanospirillum hungatei*. *Microbiology* **157**: 280–289.

Zengler, K., and Zaramela, L. S. (2018) The social network of microorganisms — how auxotrophies shape complex communities. *Nat Rev Microbiol* **16**: 383–390.

Supporting Information

Additional Supporting Information may be found in the online version of this article at the publisher's web-site:

Table S1. Genome statistics

Table S2. Transcriptome statistics

Table S3. Gene annotation of propionate catabolis, hydrogen/formate generation and electron transduction pathways.

Table S4. Gene expression levels for *P. schinkii* HH in co-culture with JF-1 in terms of reads per kilobase transcript per million mapped reads normalized to the median.

Table S5. Gene expression levels for *M. hungatei* JF-1 in co-culture with *P. schinkii* HH (left) and in axenic culture (right) in terms of reads per kilobase transcript per million mapped reads normalized to the median. The ratio of the expression and *p*-value of each gene in co-culture against axenic culture is shown ($p < 0.05$ coloured yellow). **p*-value calculated from replicate 1 and 3 of the co-culture and all replicates of the axenic culture ($p < 0.05$ coloured blue). This may be justifiable as the standard deviation of the replicate 1 and 3 is less than that of all three replicates for 82% of the JF-1 genes with detected expression. In addition, the standard deviation of replicates 1 and 3 is less than any other combination (i.e., rep. 1 + 2, 2 + 3 and 1 + 2 + 3) for 70% of the JF-1 genes with detected expression.

Table S6. Gene expression levels for *M. hungatei* JF-1 in an axenic culture in terms of reads per kilobase transcript per million mapped reads normalized to the median.

Table S7. Other catabolic/fermentation pathways found in the *P. schinkii* HH genome and the corresponding genes' average expression level (RPKM) during syntrophic propionate degradation.